A potential clue of IL-17A as a helper assist paraquat and T cell infiltration into brain parenchyma

Ge Shi
Ningxia Medical University
Kaidong Wang
Ningxia Medical University
Rong Hu
Ningxia Medical University
Yang Li
Ningxia Medical University
Yuxuan Jiao
Ningxia Medical University
Yonghang Li
Ningxia Medical University
Yujing Li
Ningxia Medical University
Ai Qi
Ningxia Medical University
Min Huang
hmin81@163.com

Ningxia Medical University

Research Article

Keywords: Paraquat, Blood-Brain-Barrier, Th17 cell, IL-17A, Neurotoxicity

Posted Date: July 3rd, 2024

DOI: https://doi.org/10.21203/rs.3.rs-4564399/v1

Additional Declarations: No competing interests reported.

A potential clue of IL-17A as a helper assist paraquat and T cell infiltration into brain parenchyma

Ge Shi [1, 2, #], Kaidong Wang [1, 2, #], Rong Hu[1, 2], Yang Li[1, 2], Yuxuan Jiao [1, 2], Yonghang Li[1, 2], Yujing Li [1, 2], Ai Qi[1, 2, *], Min Huang [1, 2, *]

[1] School of Public Health, Ningxia Medical University

[2] Key Laboratory of Environmental Factors and Chronic Disease Control, No.1160, the Street of Shengli, Xingqing District, Yinchuan, Ningxia

[#] *Ge Shi and Kaidong Wang contributed equally to this work.*

**Corresponding author: E-mail addresses: hmin81@163.com (Min Huang). qiai168@163.com (Ai Qi),*

Abstract

Paraquat (PQ), a globally widely used and highly residual herbicide, is one of the potential environmental risk factors for neurodegenerative diseases (NDs). Before exerting neurotoxicity, however, PQ needs to break through the blood-brain barrier (BBB), how it penetrates the BBB and reaches the brain parenchyma remains a mystery. Recently, peripheral T cells and cytokine infiltrates into the brain have been involved in the development of NDs. But, the main reason for the infiltrating is not yet unrevealed. BBB plays a crucial role in the communication of T cells between the central nervous system (CNS) and the peripheral. Hence, whether T cells and their cytokines serve as core assistants to assist PQ infiltrating the BBB exerting neurotoxicity, in this article, C57BL/6J mice treated with PQ experienced down emotion and learning and memory abilities decreased. Pathologically, neurons and microglia respectively exhibit selective spatial damage and hyperresponsiveness. Simultaneously there were capture the traces of CD3 and its subsets of CD4/8, as well as IL-17A. Surprisingly, the response of T cells from peripheral blood and spleen to PQ gradually leans towards Th17 cells and secretes IL-17A. Therefore, it is highly suspected that IL-17A plays a role in disrupting the BBB. In vitro, bEnd.3 cells were specifically constructed with IL-17A, and PQ or mixture revealed IL-17A takes part in PQ-induced BBB disruption. Altogether, PQ responds to peripheral T cells to react and secrete IL-17A, which destroys BBB and assists PQ and T cells or other factors in infiltrating brain parenchyma.

Graphical Abstract

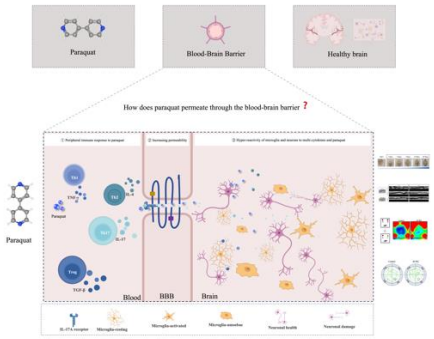

Highlights

- The increased secretion of IL-17A highly responds to PQ exposed continuously.
- IL-17A is a helper for paraquat by through blood-brain barrier.
- CD4/8 and IL-17A all reach the brain parenchyma after blood-brain barrier damage.

Abbreviations

AD: Alzheimer's disease; BBB: Blood-Brain-Barrier; CNS: Central nervous system; DEGs: Differential expression genes; DI: Discrimination index; EPA: United States Environmental Protection Agency; EB: Evans blue; FC: Flow Cytometry; GO: Gene Ontology; GWASs: Genome-wide association analyses; Hi: Hippocampus; IF: Immunofluorescent staining; IHC: Immunohistochemistry; IL-17A: Interleukin 17A; MOF: Multiple organ failure; MW: Molecular weight; MWM: Morris Water Maze; NDs: Neurodegenerative diseases; NOR: New object recognition; OB: olfactory bulb; PD: Parkinson's disease; PQ: Paraquat; SEM: Standard error of the mean; SN: Substantia nigra.

Keywords

Paraquat; Blood-Brain-Barrier; Th17 cell; IL-17A; Neurotoxicity.

1. Introduction

Pesticides can be absorbed in daily life through contact with aerosols (skin, respiratory tract) or ingested through a person's digestive tract with food. Paraquat (PQ) is one of the most widely used herbicides in the world, and it is well-known in the pesticide fields. However, acute exposure causes of multiple organ failure (MOF) eventually the strong lethality [1]. As a result, there is controversy over whether PQ is allowed to be used in the agricultural sector [2]. Although China has banned PQ from agricultural land, is still a manufacturer and exporter of PQ around the world (approximately 70 countries) [3]. Reported that PQ belongs to quick-to-kill weeds and can be quickly inactivity in soil. With the development of the detection sensor upgrading, its sensitivity has gradually increased. Nowadays, the prototype of PQ can be detected in both soil and water, indicating that PQ is not degraded and exists in water or soil in its original form [4]. PQ indirectly through the air, water, soil, and

food become diffuse and permanent pollution and then enter the organism to harm the health of humanity. At the same time, long-term exposure to PQ, especially at low doses, can also cause cumulative effects, and the current study has clarified the correlation between long-term exposure to paraquat and Parkinson's disease [5] [6]. It can be seen that PQ exposure has become one of the potential environmental risk factors for PD, but the toxic mechanism of PQ is still unclear. In vivo, PQ has been constructed to simulate Parkinson-like symptoms models in rodents, revealing a vicious cycle of progressive neuronal damage, and neuroinflammation induced by microglial activation[7, 8]. Which provided a foundation to research the neurotoxicity of PQ.

Blood-brain barrier (BBB), a highly selective filtering "layer", which allows beneficial substances to pass through while keeping harmful remaining the blood vessels. The integrity of the cerebrovascular system is also regulated by the BBB, which serves as the interface between nerve tissue and blood. Endothelial cells, along with the basal membrane, astrocyte terminal feet, and pericytes consist main components of the BBB, among which the barrier function is mainly achieved by endothelial cells [9]. However, BBB disruption is associated with a variety of central nervous system (CNS) diseases, including stroke, Alzheimer's disease (AD), and PD [10]. Additionally, the destruction also makes exogenous compounds and peripheral blood cytokines take the opportunity to invade, aggravating the deterioration of these diseases. Studies have shown that depending on the physiological structure of BBB, it effectively hurdles 98% of small-molecule drugs and almost 100% of large-molecule drugs. PQ reportedly is essentially a hydrophilic compound [11], if fully penetrates the BBB, which does not meet the conditions. Current researches are still stuck in the hypothesizes of transporter, or amino acid transport [12] [13]. However, the latest clues strongly hint that cytokines in the peripheral immune response may be the culprit in disrupting the blood-brain barrier [14] [15].

Interleukin 17A (IL-17A) is the signature cytokine of a subset of $CD4^+$ helper T cells known as Th17 cells. In the pathogenesis of AD, it has been confirmed that CD4 penetrates the brain parenchyma by differentiating into (Th17) cells and secreting IL-17A, resulting in increased levels of IL-17 and other cytokines in the cerebrospinal fluid (CSF), serum and hippocampus of AD models [16]. Interestingly, infiltrated-Th17 cells and IL-17A also penetrate leading to activation of microglia and neuronal apoptosis which exacerbates neuroinflammation and neurodegeneration [17]. Previous studies have confirmed that PQ exposure can cause an increase in IL-17A expression in the lung tissue of target organs in mice. However, there is currently no research on the relationship between the changes in IL-17A after PQ exposure and BBB damage, leading to secondary neurotoxicity and CNS diseases. Furthermore, does PQ rely on the help of peripheral IL-17A to penetrate the brain parenchyma?

The purpose of this article is to investigate the relationship between PQ and blood-brain barrier disruption and IL-17A.

2. Materials and methods

2.1 Animals

Male mice C57BL/6J (22 ± 2 g) were purchased from the Experimental Animal Centre of Ningxia Medical University, in accordance with experimental animal ethics rules (IACUC-NYLAC-2022-183), all were regularly bred in specific pathogen-free conditions under the temperature of 22±1°C and maintained on a 12-hour light cycle, and were randomly divided into 10 groups (Control, PQ-model timeline). Paraquat dichloride (analytical standard, Sigma-Aldrich, USA) for administration.

2.2 In vivo PQ-treated mouse models

Mice were treated with PQ (CAS:75365-73-0, Sigma USA) in 1.25 mg/kg via intraperitoneal injection (i.p), which according to previous research about the dosage and method of PQ [18]. Based on our previous optimal dosage triggered the classical complement cascade response in the brain of mice [19]. An equal volume of 0.9% saline for the control group.

The timeline model treatment to mice

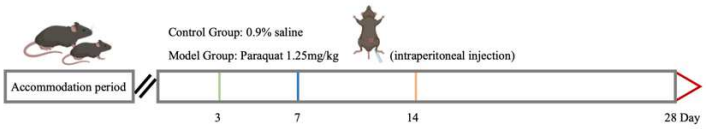

2.2 Behavioral testing

2.2.1 Pole test

The equipment consists of lengths of 50 cm upper with a ball (a diameter of 1cm). Mouse were faced upwards on the top of the pole. Which usually naturally orient downwards and descend along the length of the pole to return to their cage. In three experiments, record the time it takes for the mouse to face from upwards to downwards (T_1) and descend to the bottom of the pole (T_2).

2.2.2 New object recognition (NOR)

The equipment consists of a grey box (45 cm × 25cm × 25cm) and object 1, object 2 (objects 1 and 2 have to be the same), and object 3.

Adaptive phase: Mice severally were acclimatized in the box for five minutes.

On the first day: Mice in the box with two objects 1 and 2. Recording within ten minutes that the mouse is familiar with two objects 1 and the exploration trajectory.

The next day: Mice in the box with object 1 and object 3. Recording the exploration trajectory and duration of mice on objects 1 (F) and 3 (N) within ten minutes. The discrimination index (DI) of the mouse against object 3 is calculated. DI = (N-F) / (N + F) ×100%

2.2.3 Morris Water Maze (MWM)

The equipment consists of a circular pool (1.2 m in diameter) with a platform and positioning indicators around the pool, and a camera at the top of the pool to collect information and connect to the analysis system.

Training period: In the water maze experiment, each mouse was tested four times a day. The mice were put into the water facing the wall from the four quadrilateral entry points in a clockwise sequence, and the transparent platform was placed in the SE quadrant, with the water surface about 1 cm above the platform. During the whole process, make sure the mice can't see the platform with the naked eye, and the same mouse is tested 10 minutes apart.

Testing period: The mice entered the water from the NW quadrant, observed and recorded the number of times the mice crossed the platform and the SE time within the 60s. (Note: The platform should be removed during this experiment).

2.3 Immunity cells sorting in brain

Post PQ injection, mice were deeply anesthetized with isoflurane and then transcardially perfused with pre-freezing PBS for 5 min. Brain tissue was minced into small pieces and mechanically ground subsequently collecting the grinding solution. 30% Percoll (Cytiva; 1708910) was carried to gradient centrifugation (acceleration of 3 and deceleration of 2) for 40 min to remove myelin. The bottom contains monocyte suspension collected for subsequent experimental processes.

2.4 Flow cytometry

Samples were constantly handled on ice or at 4 °C avoiding direct light exposure during the whole process. First, samples were incubated with TruStain fcX™ anti-mouse CD16/32 to block FcγRIII/II and reduce unspecific antibody binding for 20 min. Next, samples were incubated with Zombie AquaTM Live/Dead Fixable (Biolegend) in PBS for 20 min to exclude nonviable cells. Then, incubated for 30 min with an antibody cocktail in Stain Buffer. For cell surface antigens the following table. For intracellular Foxp3/Transcription Factor staining, True-Nuclear™ Transcription Factor Buffer Set (#424401, Biolegend) was used for fixation and membrane rupture, following the manufacturer's instructions. For intracellular antigens, PE anti-mouse Foxp3 was used. For intracellular IL-17A staining, samples were incubated with Cell Activation Cocktail (with Brefeldin A) for 5 h in the constant-temperature incubator (37°C, 50% CO_2). Next incubated with Fixation Buffer (#420801, Biolegend) for 20 min and used for Intracellular Staining Perm Wash Buffer after the same surface antibody treatment step. For intracellular antigens, Brilliant Violet 421m anti-mouse IL-17A was used. Suspensions were acquired using a BD FACSCelesta. Data were analyzed with FlowJo software. Gates were set based on FMO (fluorescence minus one) controls and back-gating analysis. Percentages on cytograms were given as the percentage of a parental gate. For reagent specifications, catalog numbers, and dilutions see Table 1.

2.5 Bulk RNA-seq library preparation

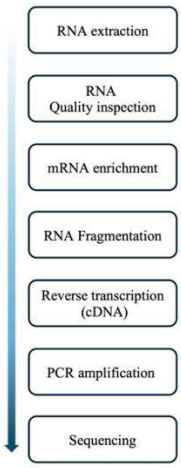

2.6 Bulk RNA-seq analysis

The transcriptome sequencing and analysis were conducted by OE Biotech Co., Ltd. (Shanghai, China). The libraries were sequenced on a llumina Novaseq 6000 platform and 150 bp paired-end reads were generated. Raw reads of fastq [20] format was firstly processed using fastp and the low-quality reads were removed to obtain the clean reads. Differential expression (DE) analysis was performed using the DESeq2 [21]. Q value < 0.05 and foldchange > 2 or foldchange < 0.5 were set as the threshold for significantly differential expression genes (DEGs). Hierarchical cluster analysis of DEGs was performed using R (v 3.2.0) to demonstrate the expression pattern of genes in different groups and samples. The radar map of the top 30 genes was drawn to show the expression of up-regulated or down-regulated DEGs using R packet ggradar. Based on the hypergeometric distribution, GO [22] pathway, and enrichment analysis of DEGs were performed to screen the significantly enriched term using R (v 3.2.0), respectively. R (v 3.2.0) was used to draw the column diagram, the chord diagram, and the Volcano map of the significant enrichment term.

2.7 Immunohistochemistry (IHC)

Post PQ injection, all mice were deeply anesthetized with isoflurane and then transcardially perfused with saline (3 min) and 4% paraformaldehyde solution (5 min). Briefly, after the collected brain tissue was sliced by paraffin embedding. Sections were dewaxed to water in a series of processes and, subsequently, carried on microwave thermal repair with sodium citrate (PH 6.0) and endogenous blocking with 0.3% peroxidase for 15 min. And were blocked with goat serum for 1 h. Then were incubated with the corresponding primary antibodies at 4 °C overnight. And incubated with secondary antibodies at room temperature for 1h. DAB chromogen solutions were added to cover the entire section. Identification of cell nucleus in Mayer's Hematoxylin Stain (G1080, Solarbio, China). Washed in deionized water and drain the slides. Visualize staining under microscopy with a bright-field illumination (Leica Instruments, Heidelberg, Germany).

2.8 Evans assay

Evans blue dye was purchased from Solarbio (CAS:314-13-6, Beijing, China) and applied to BBB integrity evaluated after PQ exposure respectively at 1, 3, 7, 14, and 28 days. According to the manufacturer's instructions, the mice were injected into the tail vein in proportion (20 μl/10g). The observation that the eyes of the mice turned blue within a short time indicated that the injection was successful. The mice were euthanized one hour later. The whole brain was collected, and the color changes of the brain tissue were observed. Subsequently, the brain tissue was quickly homogenized with 50% trichloroacetic acid within 1× PBS and centrifuged (10000 g × 20 min). The standard curve was drawn, and the Evans content was determined.

2.9 Culturing and administration cells

Resuscitated and cultured b End.3 cells to the logarithmic phase for intervention with PQ and IL-17A (Recombinant Mouse, 576004, Biolegend) which were diluted to gradient concentration for screening optimum with CCK-8 assay (HY-K0301, MCE, Shanghai China) detect the absorbance values at 450nm. Cell suspension was divided into the medium, PQ, IL-17A, and PQ+IL-17A mixture group then inoculated on a Transwell chamber with 0.4 μm aperture. The chamber was inserted into a 12-well cell culture plate in the lower chamber within 1 ml DMEM medium. After periods, discarding medium of Transwell upper and lower chamber, respectively add 1 ml DMEM medium to each lower chamber, and add 200 μl (PQ (200 μmol/l), and IL-17A (100ng/ml) and the mixture of PQ+IL-17A) to the lower chamber (200 μmol/l) cultured for 24 hours. Removing the intervention subsequently adding 200 μl EB-BSA (0.67 mg/ml) to the upper chamber which is used to ensure that the liquid level in the upper and lower chambers is consistent. Continue to cultivate for 1 hour in the incubator at 37 ℃ and 5% CO_2. Collect the EB leakage solution in the lower chamber for concentration detection after 1 hour.

2.10 Western blotting assay

Brain tissues were lysed by a cell lysator for 10 minutes then centrifuged at 12000*g* for 5 min at 4°C to collect cell suspension. Protein quantification was performed using the BCA kit (KGPBCA, Jiangsu, China) according to the supplier’s instructions. In order, the protein was transferred to the PVDF membrane after SDS-PAGE electrophoresis, followed by sealing with 5% skim milk, and incubation of primary antibody overnight. The next day, membranes were washed with PBST for 30 min, then incubated with HRP conjugated secondary antibody and subsequently imaged using ECL (Invitrogen, USA) under the Thermofisher iBright Imaging System. Finally, the quantification of the band density was determined by densitometric analysis.

Table 1 The table of antibodies used in the experiments.

Anti-body	Cat #	Dilution ratio				Company
		WB	IHC	IF	FCS	
Foxp3	#320007	-	-	-	1:100	BioLegend
IL-17A	#506925	-	-	-	1:100	BioLegend
CD3	#100327	-	-	-	1:100	BioLegend
CD4	#100509	-	-	-	1:100	BioLegend
CD8	#100713	-	-	-	1:100	BioLegend
CD45	#103127	-	-	-	1:100	BioLegend
CD25	#102011	-	-	-	1:100	BioLegend
IL-4	#504105	-	-	-	1:100	BioLegend
IFN-γ	#505839	-	-	-	1:100	BioLegend
anti-CD4	SC-19641	-	-	1:200	-	Santa Cruz, USA
anti-NEUN	ab279296	-	1:200	-	-	Abcam, USA
anti-IL-17A	ab81283	1:1000	-	-	-	Abcam, USA
anti-IL-17RA	ab179463	1:1000	-	-	-	Abcam, USA
anti-Occludin	sc-17844	1:1000	-	-	-	Santa Cruz, USA
anti-Claudin-5	ab129068	1:1000	-	-	-	Abcam, USA
anti-β-actin	20536-1-AP	1:1000	-	-	-	Proteintech, China
anti-rabbit HRP	SA00001-2	1:10000	-	-	-	Proteintech, China
anti-mouse HRP	SA00001-1	1:10000	-	-	-	Proteintech, China
anti-rabbit IgG DyLight 549	A23320	-	-	1:500	-	Abbkine, China
goat anti-mouse IgG DyLight 488	A23210	-	-	1:500	-	Abbkine, China
goat anti-rat IgG DyLight 649	A23640	-	-	1:500	-	Abbkine, China

2.11 Statistical Analysis

All data was analyzed using GraphPad Prism software (Prism 9.0, GP9-2594058-RLTV-FFFDO). For each independent experiment, include at least three to six replicates in each group. We performed simple statistical comparisons using Student's t-test, and ANOVA (one-way and two-way) was used to statistically analyze the experimental groups' data with multiple comparisons. Unpaired or paired Student's t-tests were used to compare the two groups. The significance level was set at $^{*}P < 0.05$. Data is presented with means ± standard error of the mean (SEM) shown as line and whiskers.

3. Result

3.1 Peripheral immune fluctuating responses to experiencing PQ continuous intervention

The immune system, as the "military and police" of the body, prevents external chemical invasion by adopting various forms of struggle to carry out immune responses. Toxicokinetics has revealed that when short time and acute exposure to PQ which could quickly distribute and absorb into the bloodstream in a transient time, further finally attacking target organs until whole exhaustion [23]. In this study, PQ was continuously treated (1.25mg/kg) for 28 days without having any effect on the general vital signs of mice (showing a uniform increase in mouse weight) (Fig S1 A). Spleen, as a peripheral immune organ, the organ coefficient without effect on continuous treatment PQ for 14 days.

Miraculously, the index was significantly decreased post-continuous administration with PQ for 28 days, compared with the saline group (Fig S1 B). Likewise, HE-staining demonstrated a clear boundary between the red and white pulp when PQ treatment for 3 days and 7 days, which was consistent with the control group. The boundary was somewhat unclear even diffuse after being consecutively treated for 14 days and 28 days, and the latter group was more pronounced (as shown in the white concentric circle) (Figure 1 A). It suggests PQ can cause slight damage to the spleen. Combined with flow cytometry (FC), the percentage of $CD45^+CD3^+$ labeled cells in splenic T lymphocytes did little fluctuate between PQ and saline groups (Figure 1 B). For peripheral blood T lymphocytes, however, continuous exposure to PQ for 28 days showed a significant increase in overall T cell levels, compared with the control group (P=0.0131) (Fig S1C and D). It so happened to confirm the toxicokinetics of PQ conform to blood distribution and prefer to cause an impact on peripheral blood. Further analysis of the ratio of T-cell subsets $CD4^+$ and $CD8^+$ showed a decreased level in the spleen and an increase in peripheral blood, compared to the control group (Figure 1 D and F). Altogether, the fluctuation of peripheral immune responses means immune dysfunction in mice after PQ exposure.

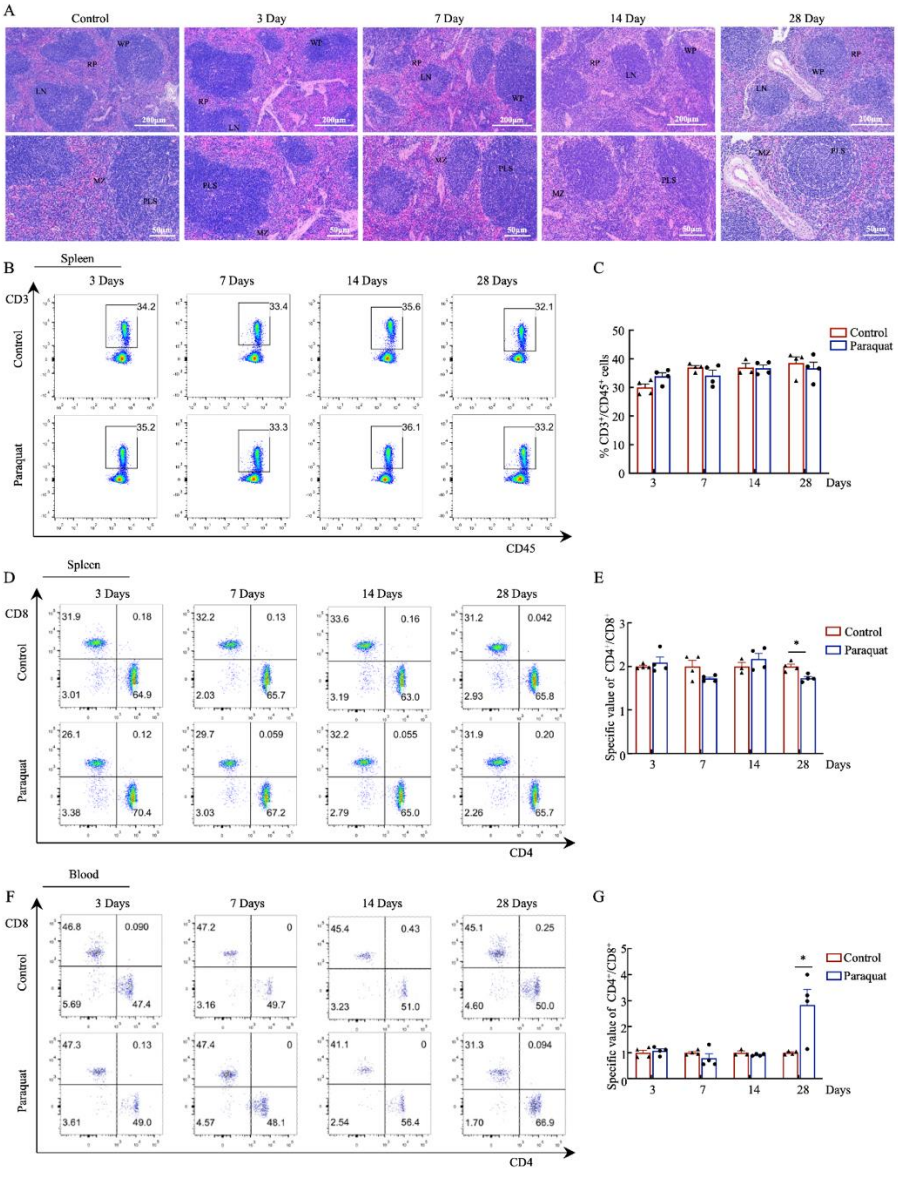

241

242 **Figure 1. PQ triggered peripheral immune responses.** (A) H&E staining of spleens, images representative.
243 Scale bar, 200 μm (upper) and 50 μm (below). WP: white pulp; RP: red pulp; LN: lymph node; PLS: periarterial lymphatic
244 sheath; MZ: marginal zone. (B) Flow cytometry analysis of the distribution of the T cell in the spleen marked with $CD45^+CD3^+$
245 cells, (C) Chart demonstrates the percentage of $CD45^+CD3^+$ cells belonging to the defined populations. Flow cytometry analysis
246 of the distribution of the T cell subsets in the spleen(D) and blood (F) marked with $CD8^+CD4^+$ cells. Gram demonstrates the ratio
247 of $CD4^+$ T to $CD8^+$ T cells in the spleen(E) and blood (G), * indicates the statistical difference in the 28-PQ group compared with
248 control (P=0.0063; 0.0234). Data are presented as means ± SEM, between two groups both the PQ model group and the control
249 group were analyzed by single-factor unpaired T-test. *: $P<0.05$.

250 **3.2 PQ caused the peripheral T cells to be inclined to Th17 differentiate and secrete IL-17A**

251 Considering $CD4^+$T cells differentiate into subtypes when accepting the signal from antigenic
252 stimulation, which is mainly divided into four characterized by markerable secretion of cytokines and
253 expression of transcription factors: Th1 cell (IFN-γ), Th2 cell (IL-4), Th17 cell (IL-17), and Treg cell
254 (Foxp3). Where in the spleen, there were varying degrees of changes in the four cytokines, differently
255 the expression level of IL-4 in the spleen showed a time-dependent increase (Fig S2 A, B, and G, H). It

indicates that the immune system has activated transfer into a defense state when receiving an unsafe sign. IL-17A also shows a significant time-dependent increase which reaches peak value within 7 days followed by a gradual decrease but still higher than the control group level (Fig 2 A, C). Conversely, the corresponding immunosuppressive factor Foxp3, showed a gradually decreased trend. There was a similar to IL-17A upping the peak value within 7 days which may also exert the role of check and balance (Fig S2 C, I). Equally, cytokine changes in the blood are also like those observed in the spleen (Fig S2 D-F, J-L). Of note, there is a slight deviation in the performance trend of blood and spleen, which may be related to individual differences in mice. Unexpectedly, the expression level of IL-17A in the blood reaches its peak in 7 days, and there is a decrease in the level with continuous PQ administrated, but it is still at a high level compared to the control group (Fig 2 B, D). Consistent with the results of FC, immune cytokine markers in peripheral serum detected with ELISA were performed TNF- γ (Th1) and IL-4 (Th2) were not significantly affected by PQ (Fig 2 E, F). For IL-17A (Th7) and TGF- β (Treg) both showed strongly opposite performances especially at 7 day which consistent with FC presentation (Fig 2 G, H). Altogether, the alteration of IL-17A levels is strong feedback on PQ exposure.

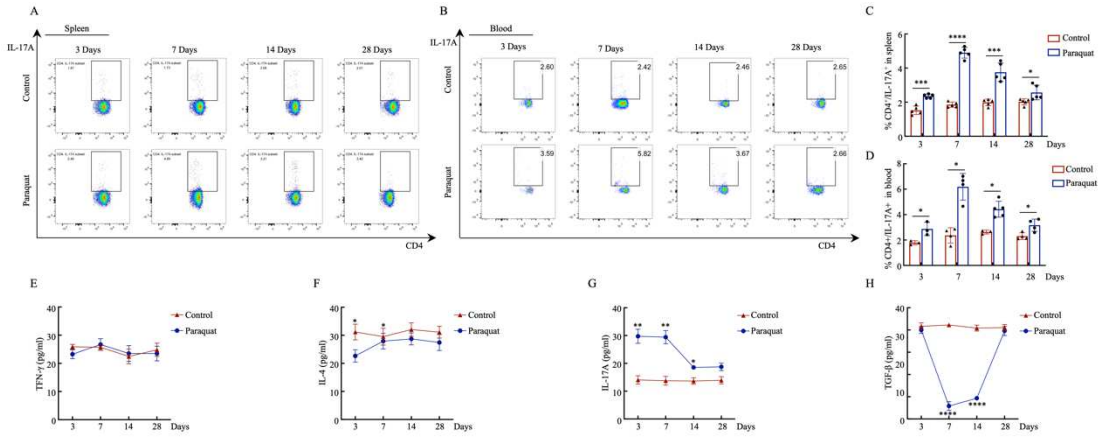

Figure 2. The inclining of T cells to Th17 differentiation after PQ exposure.

(A) Flow cytometry analysis of the distribution of IL-17A (Th17) in the subtypes of T cells in the spleen and blood (B). Histogram demonstrates the proportion of IL-17A in the spleen (C) and blood (D). (E-H) Trend line chart with ELSA detects blood serum for TNF-γ, IL-4, IL-17A, and TGF-β after PQ exposure. Data are presented as means ± SEM and were analyzed by single-factor unpaired T-test and one-way ANOVA analysis of variance. *&**&***&****represents $P < 0.05$&0.01&0.001&0.0001, compared with each group analyzed by Tukey's test for post-hoc analysis.

3.3 Microglial hyper-response and T-cell trace seized in mice brain after PQ exposure

Neuroimmunity response and neuroinflammation are regarded as the body's initial defense response, and long-term or excessive inflammation is the main cause of the development of various neurological diseases, especially NDs[24]. Microglia, the innate immune cells in the brain, are highly dynamic cells with multiple steady-state functions. Mainly participates in innate immune responses to the primary

defense system for various stresses and injuries in the central nervous system. For NDs, microglia predominantly protect the brain through rapid immune activation to maintain the homeostasis of the brain microenvironment [25]. Under emergency conditions, the morphology of microglia (resting branching type) rapidly transitions from morphological branching to, activated-type, amoebae (debranching phenotype with shorter protrusions) (Figure 3 A). After sholling analysis, intersection points of microglial branches with distance from the soma. In every brain region of PQ group, all intersection points were decreased compared to control groups (Figure 3 B). In addition, the heat map of cell transcriptome differential analysis showed that CD36 the phagocytic recognition receptor in microglia was downregulated (Figure 3 D). Which indicates microglia have initiated the defense phase.

Innate immunity and adaptive immunity form a harmonious immune balance system, under physiologically balanced conditions, the adaptive immune system also participates in maintaining homeostasis [26]. However, studies have shown that adaptive immune cell infiltration dominated by T lymphocytes promotes NDs and aging [27]. During the experimental process, we were curious about whether T cells were involved in adaptive immune responses after exposure to PQ. Firstly, flow cytometry results showed T cells with $CD45^+/CD3^+$ co-labeled were increased compared to the control group (Figure 3 C and D). At the same time, CD4 and CD8 of the T cell subsets, as well as chemokine CCL2 expression were upregulated showed in the transcriptome heatmap (Figure 3 E). In order to further observe how PQ affects T cells to infiltrate the brain parenchyma, IHC demonstrated that the positive expression of $CD4^+$ and $CD8^+$ in the olfactory bulb (OB) and substantia nigra (SN) of the brain was significantly higher than the baseline level of the control group (Figure 3 E-G). To further explore when T cells entered the brain parenchyma, the timeline of immunofluorescence showed $CD8^+$ infiltration mount up starting at 7 days. With the extension of exposure time, the amount of expression increased, reaching a peak at 28 days (the difference was statistically significant) (Figure 3 H and I). Based on the above, except microglial response to PQ exposure, there are also captured traces of T cell infiltration which may be the culprit in accelerating neurotoxicity worthing paying more attention to.

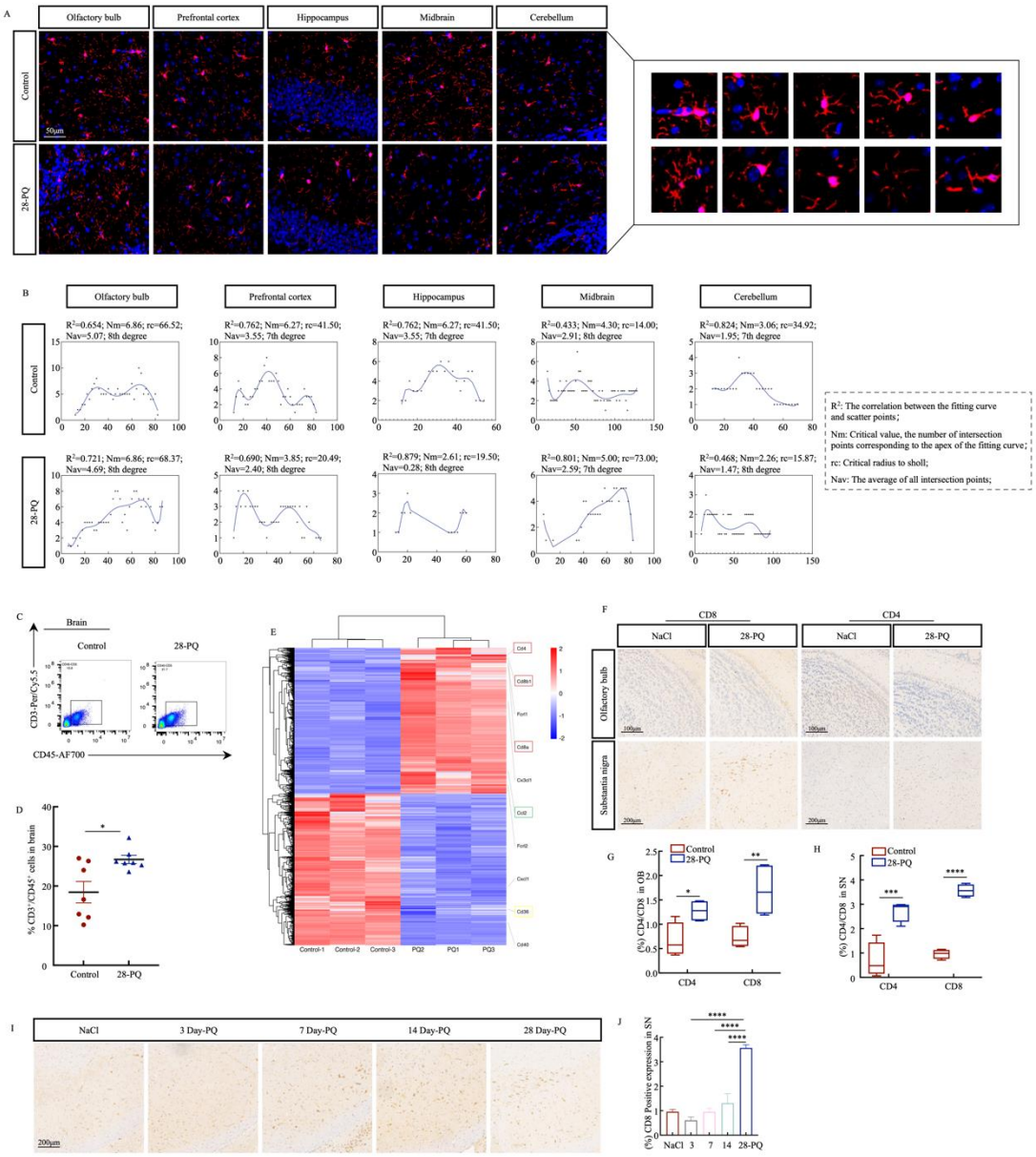

Figure 3. Abnormal microglia and T-cell infiltration were in response to PQ.

(A) Representative IF images of microglia marked with Iba-1 (red) and nucleus (DAPI) in the sagittal section of the brain. Scale bars, 50 μm. (B) Shollig analysis to intersection points of microglial branches with distance from the soma. (C) Flow cytometry analysis of the distribution of the T cell in the brain marked with $CD45^{+}CD3^{+}$ cells, (D) dot plots demonstrate the percentage of $CD45^{+}CD3^{+}$ cells belonging to the defined populations (two-sided t-test, mean ± SEM, $*P < 0.05$, P=0.014). (E) Heatmap depicting the most significant differentially expressed immune response genes of PQ treatment compared with the control including upregulation genes of T cells subset $CD4^{+}$ and $CD8^{+}$ (red rectangle) and chemokine ccl2 (green rectangle). And downregulation of microglial phagocytosis receptor CD36 (yellow rectangle) (adjusted P value < 0.05). (F) Representative immunohistochemical staining images respectively T-cell subsets from both OB and SN labeled with anti-CD4 and CD8 antibodies are showing; Scale bars, 100 μm in OB and 200 μm in SN. (G, H) Quantitative grams respectively showed the positive expression of $CD4^{+}$ and $CD8^{+}$ (%). (I) Representative images of the timeline expression of $CD8^{+}$ in SN post-PQ treatment and quantification of increasing tendency (J), Scale bars, 200 μm. Data are represented as means ± SEM.*&**&***&****represents $P < 0.05$&0.01&0.001&0. 0001, compared with each group analyzed by Tukey's test for post-hoc analysis.

3.4 Increasing permeability of BBB is the starting factor for PQ to exert neurotoxicity

Exogenous chemicals are often rapidly distributed to various target organs for a person through the ADME process. PQ has been confirmed which be highly correlated with the onset of PD, currently, PQ as well as used to simulate Parkinson's models [18]. Distinctively, we conducted continuous exposure to mice by scaling down the dose of PQ in this experiment which was further optimized based on the previous foundation [19] to be closer to the required dose of EPA[28]. The neurotoxicity of PQ was evaluated through the following behavioral tests. Primarily, the poling test was used to assess motor disorders by the total time crawling to the top and then descending to the below (Figure 4A). Of note, the PQ group spent more time arriving at the bottom than the control (Figure 4B). Morris water maze (MWM) is applied to assess spatial learning and memory, which were conducted to investigate whether continuous exposure to PQ would affect the spatial memory ability of mice. Results show starting from the third day of the positioning cruise, the escape latency of each group of mice was significantly shortened, interestingly, which gradually was significantly shorter in the PQ group than the saline on the last days ($P = 0.0468$) (Figure 4C). However, the swimming speed of PQ-exposed mice was much lower than that of the control in the periods of training (Figure 4D). On the sixth day, a trial period when the platform withdrawal test experiment, the changes in learning and memory abilities of mice in each group were observed. Results demonstrated the PQ group significantly decreased the number of times mice crossed the target platform (Figure 4E) and the proportion of time spent staying on the target platform (SE), compared with the control group ($P = 0.0373$) (Figure 4F). Moreover, during the experiment of NOR, after habituation training for object1 on the first day. Mice treated with PQ explored on object 2 spending time were significantly shorter than the control (Figure 4G). In addition, the recognition index of the control group was significantly reduced than PQ ($P = 0.0012$) (Figure 4H). Together indicates a slight decrease in autonomous activity and significant cognitive impairment under continuous exposure to PQ.

Due to the structural composition of BBB, makes it a complex passive and active structure to protect the brain from exposure to immune cells and neurotoxic exogenous. Interestingly, after staining with Evans Blue, we can visually observe that the blue color on the surface of brain tissue gradually aggravates (Fig 4I). In addition, the concentration of EB in brain tissue started to significantly increase at 7 days and showed a time-dependent increase (Fig 4J). This also indicates mice in succession exposed to PQ leading to blood-brain barrier (BBB) damage. Western blot results showed Occlaudin and Claudin-5 which were the key marker proteins of BBB were in time-dependent decline (Fig 4K-M).

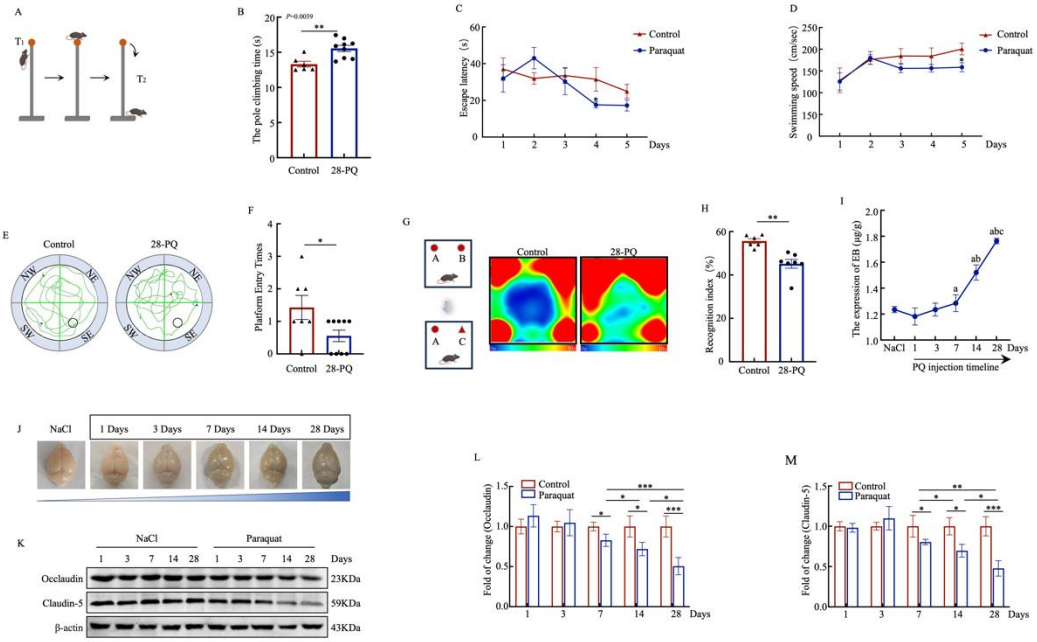

Figure 4. Low-dose paraquat exposure affected the BBB and neurological behavior of mice.

(A) Representative image of Pole climbing in which mice climbed from the bottom of the ball to the top and then descended to the bottom of the rod after PQ exposure for 28 days. (B) Quantitative histogram of time spent crawling in mice. Escape latency (C) and swimming speed (D) over the 5-day acquisition phase in the MWM test after PQ exposure (repeated-measures ANOVA). (E) Representative trajectory diagram of the MWM probe test in control and PQ-mice. (F) Histogram showed the times of mice crossed the platform. The platform is located in the SE quadrant. (G) Representative heatmaps of the NOR test in control and PQ-mice. Red zones display the areas mostly explored by the mice. (H) The quantitative evaluation of the recognition index. N = 6 to 10 mice per group. Indicator chart of EB content (I) in brain tissue and direct view of brain tissue (J) stained with EB by injecting the tail-vein of mice for 1 hour. (K-M) Immunoblotting for the expression and quantification of the tight junctional protein of BBB markers (Occlaudin and Claudin-5). β-actin was used as the internal control for normalization. Data are represented as means ± SEM.* &**represents $P < 0.05$&0.01, compared with the control group analyzed by two-sided t-test.

3.5 The neuronal abnormalities and the loss of neural synapses caused by paraquat

Golgi staining showed, compared with the control group, PQ-induced dendritic spine density in the CA1 and DG regions of the hippocampus (Hi) was significantly sparse; At the same time, there were also decreased dendritic spine in the regions of the substantia nigra (SN) (Figure 5A). Based on this, neuron further was conducted through NEUN-specific labeling. Intuitively, there was no significant difference in the positive expression of NEUN wherever was in CA1, CA3, or DG of Hi (Figure 5B and D-F). Given no changes for neurons, it is possible that neuronal activities and their responses to PQ. To assess this possibility, we investigated the expression of c-Fos, a marker of neuronal activity, in the different regions of Hi after PQ exposure [29]. In the comparison between the saline-treatment groups, immunofluorescent staining (IF) demonstrated the fluorescence intensity of c-fos-expressing co-located with NEUN was evidently weakened by PQ. It hints the neurotoxicity of PQ has already affected neuronal activity, but there has been no degree of neuronal damage (Figure 5H-J). Midbrain dopamine systems not only regulate motor but also cognitive function, and their malfunctions are

associated with increased impulsivity, and attention deficits [29]. Surprisingly, the expression level of NeuN in the SN decreased significantly (Figure 5C and G). There are spatial differences in damage for neurons that responded to PQ. We considered a Fold Change cutoff of |2| to screen for biological trends in the data which yielded 6848 genes that were differentially expressed in PQ mice compared to saline control. Pathway analysis based on Gene Ontology (GO) PopHits ≥5 includes pre/post-synaptic membrane in which 14 related genes were statistically changed, out of 13 upregulated genes (Slc family, Gabs family e.tal) and one downregulated gene Musk (Figure 5K and L). Taken together, exhibit spatial differences in neuronal activity and the expression of synaptic genes induced by PQ.

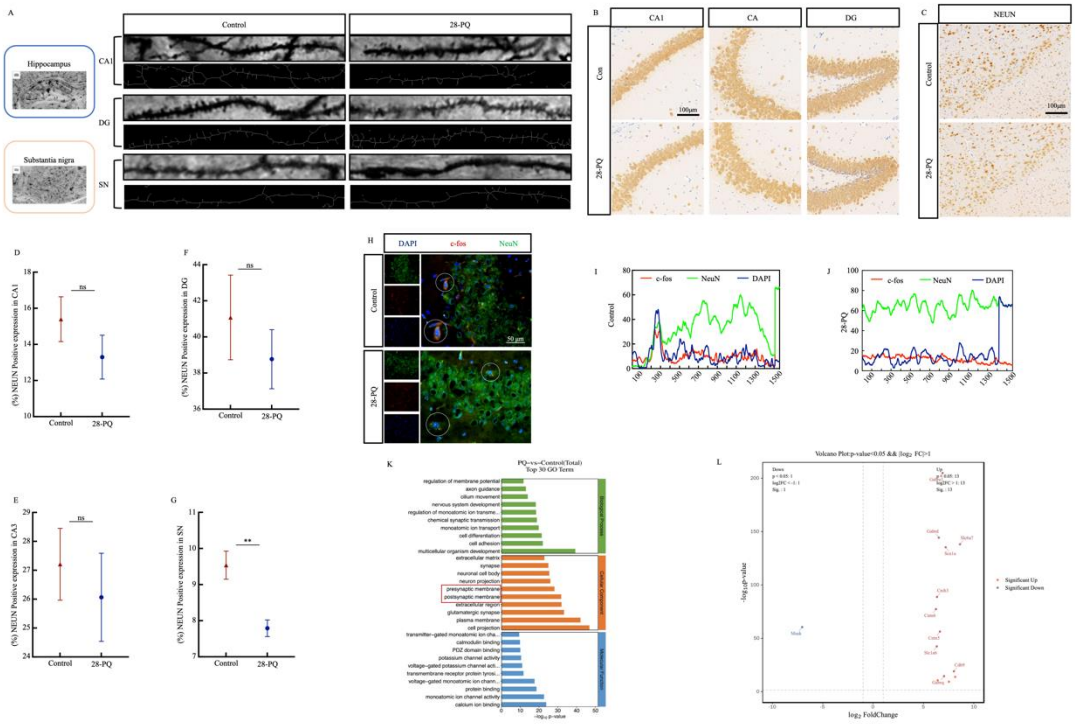

Figure 5 Paraquat affects neuronal activity and synapses in brain parenchymal neurons.

(A) Representative Golgi images of neuronal dendrites in the CA1 and DG of the hippocampus (Hi) and substantia nigra (SN). (B-C) Immunohistochemistry staining of NeuN in the CA1 and CA3 and DG of the hippocampus (left) and substantia nigra (right). Scale bars, 100 μm. Quantitative grams about the positive expression of NeuN in the CA1 (D) and CA3 (E) and DG (F) and SN (G). (H) Representative IF co-located images of c-fos (red) and NeuN (green) with nucleus (DAPI) in the CA3 of Hi. Scale bars, 50 μm. (I, J) Representative image of IF co-located coefficient among c-fos (red) and NeuN (green) with nucleus (DAPI) in the CA3 of Hi. (K) Bar plot showing GO pathways which include pre/postsynaptic membrane of the cellular component (red rectangle). (L) Volcano plot of differentially expressed (DE) genes between pre/postsynaptic membrane which were red circles the notable upregulated genes of particular interest from PQ vs control. DE was determined using an adjusted p-value (false discovery rate) <0.05. Data are represented as means ± SEM. ns represents non-statistical difference and **represents P <0.01, compared with the control group analyzed by a two-sided t-test.

3.6 IL-17A may be a helper for PQ to break through the BBB and exert neurotoxicity

Why PQ with hydrophilic structure penetrates the BBB is still a mystery. We have confirmed PQ caused the peripheral T cells inclined secrete IL-17A and T cell infiltrate into brain parenchyma. Additionally, western blot demonstrated the expression of IL-17A in brain were increasing along with

the time of PQ exposure (Figure 6A, B). Unexpectedly, the expression of IL-17A protein in the brain parenchyma showed enhanced in accordance with peripheral blood (Figure 2G). We cannot help wondering what the link of IL-17A between peripheral and brain parenchyma is. As a specific receptor for IL-17A, immunofluorescence demonstrated overlap highly between endothelial cells CD31 (red) and IL-17RA (green) in the BBB on the 7th day of PQ exposure (Fig 6C). We speculate that PQ penetrated brain parenchyma may have earlier set off the infiltration of peripheral immune cytokine IL-17A to damage BBB and seized an opportunity to enter.

To confirm the speculation, bEnd.3 cells which represent endothelial cells of BBB were conducted to treat with respectively PQ and exogenous IL-17A and both mixtures. Firstly, screened for each dose that PQ did not affect cells (0.2 μmol/l), and IL-17A had no statistically significant effect on cells (100 ng/ml) for subsequent treatment (Fig 6D and E). Evaluating the permeability of BBB in detecting the EB staining in Transwell lower chamber after administrated either separately IL-17A or PQ and combination. In the control and PQ group, it was visually observed that there was no significant EB blue staining in the lower compartment of Transwell, while treated with IL-17A and PQ+IL-17A combination were significantly blue stained (Fig 6F). Which suggests the tight structure between cells is disrupted, and EB infiltrates into the lower compartment. After quantifying the EB solution in the compartment, the EB content in the both IL-17A group and PQ+IL-17A combined group was approximately four times higher than that in the PQ-treated group and the culture medium group (Fig 6 G). Similarly, immunoblotting results showed that both IL-17A alone and in combination with PQ reduced the expression of BBB proteins (Fig 6 H-J). Immunofluorescent images of F-actin were used to label the cytoskeleton, and it was observed that the cytoskeleton structure was clear between the culture medium and PQ group, while the cytoskeleton between IL-17 and the combined PQ+IL-17A group showed blur and loose (Fig 6K). Altogether means that IL-17A acts as a risk factor triggering BBB disruption, leading to PQ taking advantage of the situation.

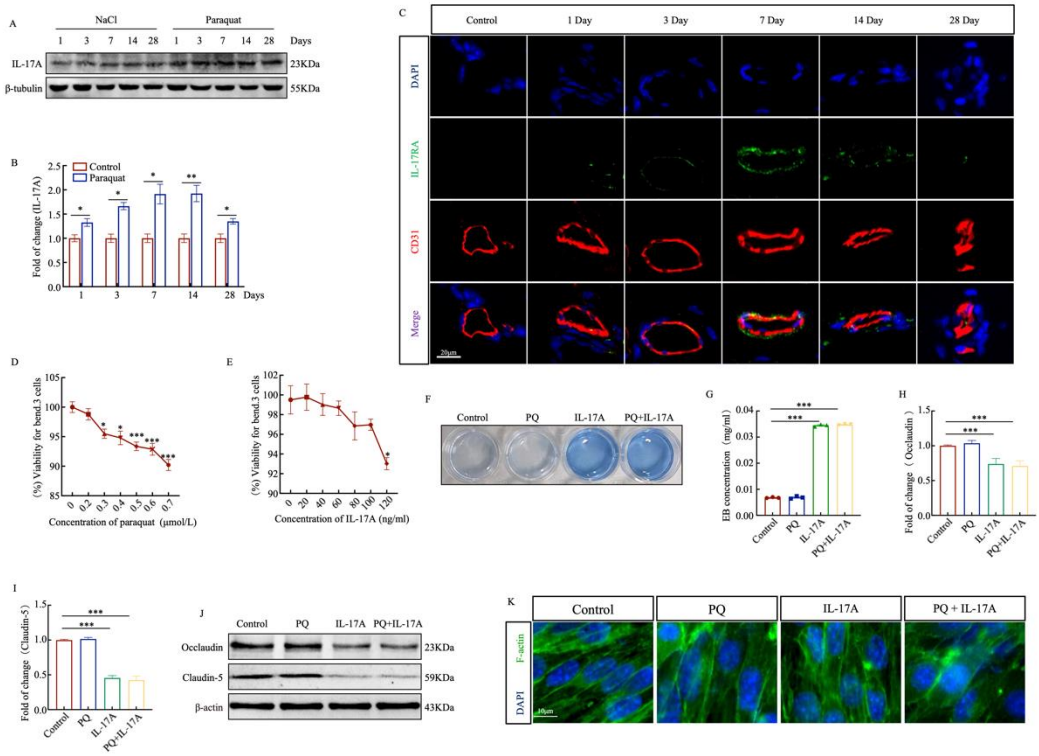

Figure 6. IL-17A is a risk factor accelerating BBB damage induced by exposure to PQ.

(A-B) Immunoblotting for the expression and quantification of the tight junctional protein of IL-17A. β-tubulin were used as the internal control for normalization. (C) Representative co-located images of CD31(vascular endothelial cells) (red) with the receptor IL-17RA (green) and nucleus (DAPI) in the sagittal section of the brain. Scale bars, 20 μm. Data are presented as means ± SEM and were analyzed by single-factor unpaired T-test and one-way ANOVA analysis of variance. *: P<0.05. ^{a}P <0.05 vs. the control group, ^{b}P <0.05 vs. the 1-Day PQ group, ^{c}P <0.05 vs. the 3-Day PQ group. Schematic showing for CCK-8 assay of the effect separately PQ (D) and IL-17A (E) in the dose-dependent on bEnd3 cell proliferation activity for 24 h, *P<0.05. Pictorial diagram of EB (F) and component (G) in the lower chamber of transwell after bEnd3 cells treated to PQ and IL-17A alone or combined estimating the permeability of monolayer endothelial cells. (H-I) Quantification of the protein expressions. (J) Immunoblotting assay was used for evaluating Occludin and Claudin-5 after bEnd3 cells were treated with PQ and IL-17A alone or combined. β-actin was used as the internal control for normalization. Data are presented as means ± SEM and was analyzed by single-factor unpaired T test and one-way ANOVA analysis of variance. *: P<0.05, **: P<0.001. (K) Representative IF images of F-actin (green) with nucleus (DAPI). The PQ group was similar to the control which was clear boundaries between the cytoskeleton of cells. Oppositively, in the IL-17A, the boundaries were unclear between cells and the PQ+IL-17A group demonstrated worse. Bars=20μm in the main images.

4. Discussion

Apart from reporting research exposing chronic PQ leading to PD, PQ is currently often preferred by the scientific community as a means of studying PD models (10mg/kg or 15 mg/kg to intermittent treatment) [30]. However, in addition to acute intentional or accidental high-dose exposure to PQ causing acute toxic effects. Actually, PQ in daily life often exists in biological media and usually poses a threat to persons with chronic exposure. The onset of PD is often a gradual and long-term process. In the early stage, we have found that the occurrence of complement cascade reactions in the mouse brain is due to continuous exposure to PQ (5mg/kg) for two weeks, which finally triggers cognitive dysfunction caused by synaptic loss in mice[19]. Therefore, in combination with EPA regulations and human surface area conversion, this experiment further lowered the dose and adopted continuous

exposure to PQ. Considering the toxicokinetic effects of PQ, the final choice was intraperitoneal (i.p.) injection[31]. Throughout the entire process, the mice all were healthy and followed the entire experimental process. Neurobehavior is a sensitive and efficient method for evaluating the neurotoxicity of chemicals. The characteristic manifestation of PD is the occurrence of motor symptoms [32]. While the exercise time of the pole climbing experiment mice was not significantly affected. During the water maze training process, however, it was found that the average swimming speed of the mice slowed down, compared with the control group. it can be concluded that has a slight impact on mouse exercise continuous exposure to PQ for 28 days, but it can be ignored. Motor symptoms are often in the late stage of a disease, and during the progression of the disease, there are often signs of non-motor symptoms such as sleep, anxiety, decreased smell, and decreased memory that patients may overlook. At the late stage of a disease, motor symptoms often develop and during the progression of the disease, there are often signs of nonmotor symptoms including sleep, anxiety, decreased smell, and decreased memory that patients may overlook[33]. Both of the experiments of MWM and NOR severally exhibited mice anxiety and depression as well as decreased learning and memory abilities. In addition, pathological validation revealed changes in dendritic spines in mouse brain parenchyma. Skeleton analysis revealed a decrease in dendritic spines. Although IHC has shown no significant difference in the reduction of NeuN within the mouse brain parenchyma. However, the image of IF of neuronal activity labeled with c-fos was slightly reduced, and combined with Go enrichment of synaptic function, significant changes were found in genes related to pre/postsynaptic membranes. Lack of Musk activity can cause synaptic structural and functional defects[34]. GABRA1, a receptor for GABA, which is an inhibitory neurotransmitter widely present in the central nervous system. Inhibiting neurons in the nervous system has neuroprotective effects and functions such as hypnosis, sedation, and anti-anxiety. The GABRD subunit will reduce the maximum current of GABAAR, increase the excitability of neuronal cells, and lead to epileptic seizures[35]. An increasing number of articles point out that exogenous chemicals can cause synaptic loss or dysfunction in the mammalian brain parenchyma, leading to cognitive impairment [36, 37]. Consequently, it can't ignore it anymore the neurotoxicity caused by chronic low-dose exposure to PQ.

Microglia, as inherent immune effector cells in the CNS, play a role in immune surveillance, nourishing neurons, regulating neural circuits, and maintaining homeostasis of the CNS. Microglia are generally divided into resting and activated states. Resting state, highly branched makes direct contact with neuronal synapses to monitor synaptic function. When a danger signal occurs, microglia quickly from rest transit activated state (amoeba-like). The activation status of microglia is closely related to the occurrence and development of various NDs and nerve injuries [38]. In this study, microglia exhibited different morphological phenotypes in different brain regions after treatment with PQ for 28 days. Compared with the control group, Microglia significantly proliferated and showed fragmented branching in the olfactory bulb area. while visibly enlarged and de-branched in size in the prefrontal lobe area. Similarly, although in the hippocampus, midbrain, and cerebellum regions, microglia exhibited similar states, the number of microglia decreased, and the fluorescence intensity weakened.

All means the response of microglia to PQ exhibits spatial heterogeneity in brain parenchyma. Neuroimmune response has also been proven to be a key trigger for NDs[39]. Innate immunity and adaptive immunity belong to the two modes of immune response. Microglia are recognized as having the main role in participating in the innate immune response.

In recent years, research has shown that in the brains of patients with NDs, in addition to the innate immunity involved in microglia, the protagonist (T cell) of the adaptive immune response has gradually been captured. Similarly, in this experiment, Flow cytometry showed a significant increase in total T cell marker $CD3^+$ in the brain parenchyma compared to the control group. Heat map enrichment of immune cells by brain parenchymal monocytes, showing T cell subsets $CD4^+$ and $CD8^+$ were also highly expressed. Research has shown that the neurotoxicity of PQ in the brain parenchyma is mainly a pathological change of dopamine neurons in the substantia nigra (SN). The distribution of ^{14}C-PQ in the brain parenchyma is twice higher in the olfactory bulb (OB) than in other brain regions (with similar average concentrations)[40]. Otherwise, there are two hypotheses about the development and origin of PD: the theory of intestinal origin and the Braak hypothesis which proposes pathology primarily involves the olfactory bulb[41]. For example, the development process of pathological protein aggregation in brain regions α-Syn from the OB transmission to a linear system[42]. In order to capture which region T cells preferentially reach, we observed strong positive expression of $CD4^+$ and $CD8^+$ in both regions OB and SN, and there was no significant difference between the two regions. To further trace back to which stage T cell infiltration occurred, it was found through a timeline that $CD8^+$ traces had already appeared after PQ exposure for 7 days until a significant infiltration appeared for treatment consecutive 28 days. Therefore, the immune response induced by PQ exposure is not only innate immunity involving microglia but also adaptive immunity involving T cells. However, it is necessary to further explore how T cells exert their toxic effects and which one of the mechanisms takes part for all special researchers.

The traditional theory suggests that PQ belongs to a water-soluble molecule, which absorbed into the blood can quickly be distributed to various tissues and organs. The lung is its main target organ and storage reservoir[43]. Additionally, the brain is known as the immune exemption zone, where T cells are hardly found. However, the function of the brain depends on adaptive immunity, and meningeal immunity maintains the brain's environmental homeostasis[44]. The integrity of the cerebral microvascular system is regulated by the BBB, which is composed of collaborative cells, connecting and transporting elements. As the interface between nerve tissue and blood, the BBB protects the brain from toxins and pathogens, as well as nerve tissue from peripheral immune cells[10]. For BBB, a key site is capillary endothelial cells which are composed bilayer membrane structure of the brain based on lipids and play an important role in controlling the entry and exit of substances into and out of cells. In other words, all elements must strictly meet the conditions allowed by BBB to pass by. Here, a wide range of lipid-soluble molecules is allowed to diffuse into the brain, mainly depending on their own lipophilicity, molecular weight (<400-500 Da), and hydrogen bonding ability (<8-10 hydrogen bonds)

and 2 <log Kow <4[45]. While PQ is extremely hydrophilic (Molecular weight, MW=257, log Kow = −4.5)[46]. So, the most fundamental factor causing T-cell infiltration due to PQ exposure is still the destruction and enhanced permeability of BBB. Nevertheless, there seems to be some contradiction when considering the differences in physical and chemical properties between PQ and BBB. Therefore, exploring the inducements of PQ on BBB permeability has become the main focus of this study. Is there a link between brain parenchymal T-cell infiltration and peripheral T-cell response?

The spleen, a hematopoietic organ in the embryonic stage finally evolves into the largest peripheral immune organ in the human body after bone marrow hematopoiesis. It is the site where mature lymphocytes settle, with T cells and B cells severally accounting for 40% and 60%. T lymphocytes are inflowed along the bloodstream and subsequently distributed to the thymus to be recycled through lymphatic vessels, peripheral blood, and tissue fluid, exerting cellular immunity and immune regulation functions. $CD3^+$ is a key marker of T cell development and maturation. Which can be divided into $CD4^+$T and $CD8^+$T lymphocytes. The former regulates or assists other lymphocytes in exerting immune functions, while the latter often exhibits cytotoxic activity [47]. The ratio of $CD4^+$T to $CD8^+$T lymphocytes changes in response to harmful substances, which means the body is in a certain immune status. When the ratio increases, may be in an "overactive" state. When the ratio decreases, it may be in an "immunosuppressive" state. Both can cause autoimmune diseases leading to adverse outcomes [48]. After being treated with 1.0mg/kg PQ for 21 days, the percentage of $CD3^+$T lymphocytes in the spleen of male Balb/c inbred mice significantly increased, while there was no significant difference in the percentage of $CD4^+$, $CD8^+$T lymphocytes, and the ratio of both[49]. In our experiment, after PQ exposure for 28 days, the percentage of $CD3^+$T lymphocytes in the spleen did not show significant changes, but the ratio of $CD4^+/CD8^+$T lymphocytes significantly decreased. While the percentage in peripheral blood significantly increased as well as the ratio increased after administration with PQ for 14 days and 28 days. It suggests short-term repeated exposure to PQ may lead to an overactive immune response mediated by peripheral blood T lymphocytes, manifested by $CD4^+$T lymphocyte levels. During this experiment, it was observed pathological damage occurred in the spleen of mice. Further flow cytometry revealed the total T cell marker by $CD3^+$ and the ratio of $CD4^+/CD8^+$ fluctuations in the spleen and blood of mice. Strangely, compared with the control group, the ratio of CD4/CD8 in the spleen increased first and then decreased in the spleen following PQ exposure. However, there was just a significant increase in the blood when continuing exposure to PQ for 28 days. This may indicate that the immune activation defense status of mice has been on.

Under different microenvironments, $CD4^+$T cells differentiate into four categories based on their cytokines and transcription factors: Th1, Th2, Th17, and Treg cells. These play an important role in resisting pathogen infection and negatively regulating immune responses. Th1/Th17 cells drive an autoimmune inflammatory process, while Th2 and Treg cells initiate immunosuppression to counteract the inflammatory response. A pair of Th17 and Treg complement each other to maintain the immune homeostasis microenvironment. During this experiment, the IL-17A secreted by Th17 cells in the

spleen with the most significant changes which increased exposure to 3 days and reached a peak when 7 days, showing a mountain-like trend. Clearly, Foxp3 showed an opposite trend with a gradual decrease. This indicates that the organism has already experienced an imbalanced immune response, gradually tending towards Th17 cell differentiation and secretion of Il-17A. The composition of BBB makes it a complex passive and active structure, protecting the brain from exposure to immune cells and neurotoxic substances. Compounds with a MW higher than 180 Da cannot penetrate the BBB. Evans Blue (EB) is an inert tracer with a MW of 961 Da, which is one of the largest commonly used dyes[50]. After injection, EB will leak through BBB and bind with albumin to form a high molecular weight complex of 68500 Da. And colored the brain areas with damaged barriers to accurately identify areas with altered permeability which can be quantitatively evaluated EB. We applied this method and intuitively observed that the color of mouse brain tissue showed a gradient deepening. Quantifying the EB content in the brain tissue homogenate, which increased when exposure 7 days and sharply increased with prolonged exposure time. IL-17A is considered a marker cytokine produced by Th17 cells which are involved in the occurrence and development of various CNS diseases[51, 52]. In vitro, Th17 cells directly promote the loss of dopaminergic neurons[17]. In vivo, can promote depressive-like behavior in mice [53]. Currently, it is believed that epithelial cells, endothelial cells, and fibroblasts are the main targets of IL-17A. Which belongs to the interleukin-17 (IL-17) families and plays a crucial role in host defense against microbial and inflammatory disease development. Pathologically, the production of IL-17A leads to excessive inflammation and significant tissue damage. The receptor families of IL-17A consist of five members (IL-17RA, RB, RC, RD, and RE). Among these, IL-17RA is a common receptor for IL-17A[54]. Reporting that IL-17A can not only promote the increase of BBB permeability[55], but also promote the migration of $CD4^{+}$T lymphocytes between BBB endothelial cells[56]. We found that PQ caused a decreased expression of tight junction proteins in the BBB of mice, with the most significant effect observed when 28 days, compared with the control group. At the same time, IL-17A showed an increased level in PQ-exposed mice, reaching a peak at 7 days and then slowly decreasing, but still higher than the control group. Strangely, which consistent with the expression trend of IL-17A in the periphery blood. Moreover, the fluorescence intensity of IL-17RA expression on the surface of CD31-labeled endothelial cells is also enhanced. Therefore, we further explore the relationship between IL-17A, and BBB was conducted. There were chosen the concentration of PQ and IL-17A had no significant concentration on bEnd.3 cell activity. Respectively respective and combined interventions were performed on the cells. Firstly, the permeability of the cells increased mainly due to EB infiltration from the upper compartment to the lower compartment of Transwell, and its content also significantly increased, between the IL-17A group and IL-17A+ PQ group have no significance. Similarly, the tight junction protein of the cells is also reduced. The F-actin-labeled cytoskeleton shows that the boundaries between cells are blurred. Overall, conjectured the increased permeability of the BBB may be mainly attributed to the main destruction of IL-17A.

The main purpose of this study is to explore the triggers for the infiltration of T cell traces in the brain parenchyma after PQ exposure, focusing on whether the disruption of the BBB is attributed to PQ or

whether it is indirectly caused by the IL-17A induced by PQ. We conclude that IL-17A alone has a higher destructive effect on the BBB than PQ alone. Of note, we did not fully confirm how IL-17A infiltration into the entire brain parenchyma after exposure to PQ, as well as the order of IL-17A and PQ to invade the BBB. In vitro, were not directly validated using IL-17A extracted from peripheral blood. The above defects still need further investigation by us to confirm that PQ postexposure IL-17A is the main culprit causing damage to BBB thereby infiltrating brain parenchyma and assisting PQ and peripheral immune factors enter.

5. Conclusion

PQ continuously exposed can lead to depression and decreased learning ability in mice, Pathologically, it can damage BBB and infiltrate T cells into the brain parenchyma. The elevation of IL-17A in peripheral blood is the primary response to PQ, and it is involved in disrupting the BBB, causing PQ and peripheral T cells to take advantage of it to infiltrate the brain parenchyma. IL-17A may be a risk factor or helper for exposure to exogenous chemicals triggering blood-brain barrier disruption.

6. Author's statement

We would like to declare on our behalf that the work described was original and has not been published elsewhere before, in whole or part. All the authors listed have no conflicts of interest and have approved the manuscript that is enclosed.

7. Authors' contributions

Study Conception and Design: Ge Shi, Min Huang; Manuscript Writing: Ge Shi; Preparation of Figures: Ai Qi, Kaidong Wang; Partial experiments undertaking: Rong Hu, Yuxuan Jiao; Data processing and figures integration: Rong Hu and Yang Li; Reference Search and Formatting: Yonghang Li and Yujing Li; Manuscript Review: Ai Qi, Min Huang. All authors read and approved the final version of the manuscript.

8. Acknowledgments

The National Natural Science Foundation of China (grant numbers 82160609, 82360649), and the Key R&D Plan of Ningxia Hui Autonomous Region [2022BEG02027] supported the present study. We sincerely thank the Ethics Committee of Ningxia Medical University.

9. Conflict of interest

All authors declare that they have no conflict of interest.

10. Reference

[1] Buckley, N. A.; Fahim, M.; Raubenheimer, J.; Gawarammana, I. B.; Eddleston, M.; Roberts, M. S.; Dawson, A. H., Case fatality of agricultural pesticides after self-poisoning in Sri Lanka: a prospective cohort study. *Lancet Glob Health* **2021,** *9* (6), e854-e862.http://dx.doi.org/10.1016/S2214-109X(21)00086-3

[2] Bang, Y. J.; Kim, J.; Lee, W. J., Paraquat use among farmers in Korea after the ban. *Arch Environ Occup Health* **2017,** *72* (4), 231-234.http://dx.doi.org/10.1080/19338244.2016.1192982

[3] US reinstates tariff exemptions on some Chinese products, including paraquat. https://news.agropages.com/News/print-42306.htm (accessed 03-24-2022).

[4] Fu, G.; Duan, Y.; Yi, W.; Zhang, S.; Liang, W.; Li, H.; Yan, H.; Wu, B.; Fu, S.; Zhang, J.; Zhang, G.; Wang, G.; Liu, Y.; Xu, S., A rapid and reliable immunochromatographic strip for detecting paraquat poinsoning in domestic water and real human samples. *Environ Pollut* **2022,** *315*, 120324.http://dx.doi.org/10.1016/j.envpol.2022.120324

[5] Kamel, F., Epidemiology. Paths from pesticides to Parkinson's. *Science (New York, N.Y.)* **2013,** *341* (6147), 722-3.http://dx.doi.org/10.1126/science.1243619

[6] Vaccari, C.; El Dib, R.; Gomaa, H.; Lopes, L. C.; de Camargo, J. L., Paraquat and Parkinson's disease: a systematic review and meta-analysis of observational studies. *J Toxicol Environ Health B Crit Rev* **2019,** *22* (5-6), 172-202.http://dx.doi.org/10.1080/10937404.2019.1659197

[7] Wu, J.; Shao, W.; Liu, X.; Zheng, F.; Wang, Y.; Cai, P.; Guo, Z.; Hu, H.; Yu, G.; Guo, J.; Yao, L.; Wu, S.; Li, H., Microglial exosomes in paraquat-induced Parkinson's disease: Neuroprotection and biomarker clues. *Environmental pollution (Barking, Essex : 1987)* **2024,** *352*, 124035.http://dx.doi.org/10.1016/j.envpol.2024.124035

[8] Shi, G.; Zhang, C.; Bai, X.; Sun, J.; Wang, K.; Meng, Q.; Li, Y.; Hu, G.; Hu, R.; Cai, Q.; Huang, M., A potential mechanism clue to the periodic storm from microglia activation and progressive neuron damage induced by paraquat exposure. *Environmental toxicology* **2024,** *39* (3), 1874-1888.http://dx.doi.org/10.1002/tox.24053

[9] Sweeney, M. D.; Zhao, Z.; Montagne, A.; Nelson, A. R.; Zlokovic, B. V., Blood-Brain Barrier: From Physiology to Disease and Back. *Physiol Rev* **2019,** *99* (1), 21-78.http://dx.doi.org/10.1152/physrev.00050.2017

[10] Chang, J.; Mancuso, M. R.; Maier, C.; Liang, X.; Yuki, K.; Yang, L.; Kwong, J. W.; Wang, J.; Rao, V.; Vallon, M.; Kosinski, C.; Zhang, J. J.; Mah, A. T.; Xu, L.; Li, L.; Gholamin, S.; Reyes, T. F.; Li, R.; Kuhnert, F.; Han, X.; Yuan, J.; Chiou, S. H.; Brettman, A. D.; Daly, L.; Corney, D. C.; Cheshier, S. H.; Shortliffe, L. D.; Wu, X.; Snyder, M.; Chan, P.; Giffard, R. G.; Chang, H. Y.; Andreasson, K.; Kuo, C. J., Gpr124 is essential for blood-brain barrier integrity in central nervous system disease. *Nature medicine* **2017,** *23* (4), 450-460.http://dx.doi.org/10.1038/nm.4309

[11] Zou, T.; He, P.; Cao, J.; Li, Z., Determination of paraquat in vegetables using HPLC-MS-MS. *J Chromatogr Sci* **2015,** *53* (2), 204-9.http://dx.doi.org/10.1093/chromsci/bmu041

[12] Shimizu, K.; Ohtaki, K.; Matsubara, K.; Aoyama, K.; Uezono, T.; Saito, O.; Suno, M.; Ogawa, K.; Hayase, N.; Kimura, K.; Shiono, H., Carrier-mediated processes in blood--brain barrier penetration and neural uptake of paraquat. *Brain Res* **2001,** *906* (1-2), 135-42.http://dx.doi.org/10.1016/s0006-8993(01)02577-x

[13] Prasad, K.; Winnik, B.; Thiruchelvam, M. J.; Buckley, B.; Mirochnitchenko, O.; Richfield, E. K., Prolonged toxicokinetics and toxicodynamics of paraquat in mouse brain. *Environ Health Perspect* **2007,** *115* (10), 1448-53.http://dx.doi.org/10.1289/ehp.9932

[14] Huang, X.; Hussain, B.; Chang, J., Peripheral inflammation and blood-brain barrier disruption: effects and mechanisms. *CNS Neurosci Ther* **2021,** *27* (1), 36-47.http://dx.doi.org/10.1111/cns.13569

[15] Nishibori, M.; Wang, D.; Ousaka, D.; Wake, H., High Mobility Group Box-1 and Blood-Brain Barrier Disruption. *Cells* **2020,** *9* (12).http://dx.doi.org/10.3390/cells9122650

[16] Chen, J.; Liu, X.; Zhong, Y., Interleukin-17A: The Key Cytokine in Neurodegenerative Diseases. *Front Aging Neurosci* **2020,** *12*, 566922.http://dx.doi.org/10.3389/fnagi.2020.566922

[17] Liu, Z.; Qiu, A. W.; Huang, Y.; Yang, Y.; Chen, J. N.; Gu, T. T.; Cao, B. B.; Qiu, Y. H.; Peng, Y. P., IL-17A exacerbates neuroinflammation and neurodegeneration by activating microglia in rodent models of Parkinson's disease. *Brain, behavior, and immunity* **2019,** *81*, 630-

645.http://dx.doi.org/10.1016/j.bbi.2019.07.026

[18] Han, S.; Feng, Y.; Guo, M.; Hao, Y.; Sun, J.; Zhao, Y.; Dong, Q.; Zhao, Y.; Cui, M., Role of OCT3 and DRP1 in the Transport of Paraquat in Astrocytes: A Mouse Study. *Environ Health Perspect* **2022,** *130* (5), 57004.http://dx.doi.org/10.1289/EHP9505

[19] Zhang, C.; Shi, G.; Li, G.; Zuo, K.; Bai, X.; Meng, Q.; Huang, M., Paraquat induces microglial cause early neuronal synaptic deficits through activation of the classical complement cascade response. *Immunobiology* **2022,** *227* (6), 152275.http://dx.doi.org/10.1016/j.imbio.2022.152275

[20] Chen, S.; Zhou, Y.; Chen, Y.; Gu, J., fastp: an ultra-fast all-in-one FASTQ preprocessor. *Bioinformatics* **2018,** *34* (17), i884-i890.http://dx.doi.org/10.1093/bioinformatics/bty560

[21] Love, M. I.; Huber, W.; Anders, S., Moderated estimation of fold change and dispersion for RNA-seq data with DESeq2. *Genome Biol* **2014,** *15* (12), 550.http://dx.doi.org/10.1186/s13059-014-0550-8

[22] The Gene Ontology, C., The Gene Ontology Resource: 20 years and still GOing strong. *Nucleic Acids Res* **2019,** *47* (D1), D330-D338.http://dx.doi.org/10.1093/nar/gky1055

[23] Qin, L.; Zhang, X.; Wu, J.; Zhang, W.; Lu, X.; Sun, H.; Zhang, J.; Guo, L.; Xie, J., Quantification and toxicokinetics of paraquat in mouse plasma and lung tissues by internal standard surface-enhanced Raman spectroscopy. *Anal Bioanal Chem* **2022,** *414* (7), 2371-2383.http://dx.doi.org/10.1007/s00216-022-03875-1

[24] Adamu, A.; Li, S.; Gao, F.; Xue, G., The role of neuroinflammation in neurodegenerative diseases: current understanding and future therapeutic targets. *Frontiers in aging neuroscience* **2024,** *16*, 1347987.http://dx.doi.org/10.3389/fnagi.2024.1347987

[25] Madore, C.; Yin, Z.; Leibowitz, J.; Butovsky, O., Microglia, Lifestyle Stress, and Neurodegeneration. *Immunity* **2020,** *52* (2), 222-240.http://dx.doi.org/10.1016/j.immuni.2019.12.003

[26] Cutolo, M.; Campitiello, R.; Gotelli, E.; Soldano, S., The Role of M1/M2 Macrophage Polarization in Rheumatoid Arthritis Synovitis. *Front Immunol* **2022,** *13*, 867260.http://dx.doi.org/10.3389/fimmu.2022.867260

[27] Jorfi, M.; Maaser-Hecker, A.; Tanzi, R. E., The neuroimmune axis of Alzheimer's disease. *Genome Med* **2023,** *15* (1), 6.http://dx.doi.org/10.1186/s13073-023-01155-w

[28] EPA Makes Paraquat Draft Risk Assessments Available for Public Comment. https://www.epa.gov/pesticides/epa-makes-paraquat-draft-risk-assessments-available-public-comment (accessed October 15, 2019).

[29] Zhang, J.; Zhang, D.; McQuade, J. S.; Behbehani, M.; Tsien, J. Z.; Xu, M., c-fos regulates neuronal excitability and survival. *Nat Genet* **2002,** *30* (4), 416-20.http://dx.doi.org/10.1038/ng859

[30] Czerniczyniec, A.; Karadayian, A. G.; Bustamante, J.; Cutrera, R. A.; Lores-Arnaiz, S., Paraquat induces behavioral changes and cortical and striatal mitochondrial dysfunction. *Free radical biology & medicine* **2011,** *51* (7), 1428-36.http://dx.doi.org/10.1016/j.freeradbiomed.2011.06.034

[31] Stevens, A. J.; Campbell, J. L., Jr.; Travis, K. Z.; Clewell, H. J., 3rd; Hinderliter, P. M.; Botham, P. A.; Cook, A. R.; Minnema, D. J.; Wolf, D. C., Paraquat pharmacokinetics in primates and extrapolation to humans. *Toxicology and applied pharmacology* **2021,** *417*, 115463.http://dx.doi.org/10.1016/j.taap.2021.115463

[32] Zhao, N.; Yang, Y.; Zhang, L.; Zhang, Q.; Balbuena, L.; Ungvari, G. S.; Zang, Y. F.; Xiang, Y. T., Quality of life in Parkinson's disease: A systematic review and meta-analysis of comparative studies. *CNS neuroscience & therapeutics* **2021,** *27* (3), 270-279.http://dx.doi.org/10.1111/cns.13549

[33] Schapira, A. H. V.; Chaudhuri, K. R.; Jenner, P., Non-motor features of Parkinson disease. *Nature reviews. Neuroscience* **2017,** *18* (7), 435-450.http://dx.doi.org/10.1038/nrn.2017.62

[34] Burden, S. J.; Yumoto, N.; Zhang, W., The role of MuSK in synapse formation and

731 neuromuscular disease. *Cold Spring Harbor perspectives in biology* **2013,** *5* (5),
732 a009167.http://dx.doi.org/10.1101/cshperspect.a009167

733 [35] Windpassinger, C.; Kroisel, P. M.; Wagner, K.; Petek, E., The human gamma-aminobutyric acid
734 A receptor delta (GABRD) gene: molecular characterisation and tissue-specific expression. *Gene* **2002,**
735 *292* (1-2), 25-31.http://dx.doi.org/10.1016/s0378-1119(02)00649-2

736 [36] Agarwal, S.; Schaefer, M. L.; Krall, C.; Johns, R. A., Isoflurane Disrupts Postsynaptic Density-
737 95 Protein Interactions Causing Neuronal Synapse Loss and Cognitive Impairment in Juvenile Mice via
738 Canonical NO-mediated Protein Kinase-G Signaling. *Anesthesiology* **2022,** *137* (2), 212-
739 231.http://dx.doi.org/10.1097/aln.0000000000004264

740 [37] Byun, Y. G.; Kim, N. S.; Kim, G.; Jeon, Y. S.; Choi, J. B.; Park, C. W.; Kim, K.; Jang, H.;
741 Kim, J.; Kim, E.; Han, Y. M.; Yoon, K. J.; Lee, S. H.; Chung, W. S., Stress induces behavioral
742 abnormalities by increasing expression of phagocytic receptor MERTK in astrocytes to promote
743 synapse phagocytosis. *Immunity* **2023,** *56* (9), 2105-
744 2120.e13.http://dx.doi.org/10.1016/j.immuni.2023.07.005

745 [38] Yang, H. M.; Wang, Y. L.; Liu, C. Y.; Zhou, Y. T.; Zhang, X. F., A time-course study of
746 microglial activation and dopaminergic neuron loss in the substantia nigra of mice with paraquat-
747 induced Parkinson's disease. *Food and chemical toxicology : an international journal published for the*
748 *British Industrial Biological Research Association* **2022,** *164*,
749 113018.http://dx.doi.org/10.1016/j.fct.2022.113018

750 [39] Scheiblich, H.; Trombly, M.; Ramirez, A.; Heneka, M. T., Neuroimmune Connections in Aging
751 and Neurodegenerative Diseases. *Trends in immunology* **2020,** *41* (4), 300-
752 312.http://dx.doi.org/10.1016/j.it.2020.02.002

753 [40] Breckenridge, C. B.; Sturgess, N. C.; Butt, M.; Wolf, J. C.; Zadory, D.; Beck, M.; Mathews, J.
754 M.; Tisdel, M. O.; Minnema, D.; Travis, K. Z.; Cook, A. R.; Botham, P. A.; Smith, L. L.,
755 Pharmacokinetic, neurochemical, stereological and neuropathological studies on the potential effects of
756 paraquat in the substantia nigra pars compacta and striatum of male C57BL/6J mice. *Neurotoxicology*
757 **2013,** *37*, 1-14.http://dx.doi.org/10.1016/j.neuro.2013.03.005

758 [41] Braak, H.; Ghebremedhin, E.; Rüb, U.; Bratzke, H.; Del Tredici, K., Stages in the development
759 of Parkinson's disease-related pathology. *Cell and tissue research* **2004,** *318* (1), 121-
760 34.http://dx.doi.org/10.1007/s00441-004-0956-9

761 [42] Sawamura, M.; Onoe, H.; Tsukada, H.; Isa, K.; Yamakado, H.; Okuda, S.; Ikuno, M.;
762 Hatanaka, Y.; Murayama, S.; Uemura, N.; Isa, T.; Takahashi, R., Lewy Body Disease Primate Model
763 with α-Synuclein Propagation from the Olfactory Bulb. *Movement disorders : official journal of the*
764 *Movement Disorder Society* **2022,** *37* (10), 2033-2044.http://dx.doi.org/10.1002/mds.29161

765 [43] Dinis-Oliveira, R. J.; Duarte, J. A.; Sánchez-Navarro, A.; Remião, F.; Bastos, M. L.; Carvalho,
766 F., Paraquat poisonings: mechanisms of lung toxicity, clinical features, and treatment. *Critical reviews*
767 *in toxicology* **2008,** *38* (1), 13-71.http://dx.doi.org/10.1080/10408440701669959

768 [44] Schwartz, M.; Cahalon, L., The vicious cycle governing the brain-immune system relationship in
769 neurodegenerative diseases. *Current opinion in immunology* **2022,** *76*,
770 102182.http://dx.doi.org/10.1016/j.coi.2022.102182

771 [45] Pandit, R.; Chen, L.; Götz, J., The blood-brain barrier: Physiology and strategies for drug
772 delivery. *Advanced drug delivery reviews* **2020,** *165-166*, 1-
773 14.http://dx.doi.org/10.1016/j.addr.2019.11.009

774 [46] Brand, R. M.; Charron, A. R.; Dutton, L.; Gavlik, T. L.; Mueller, C.; Hamel, F. G.;
775 Chakkalakal, D.; Donohue, T. M., Jr., Effects of chronic alcohol consumption on dermal penetration of
776 pesticides in rats. *Journal of toxicology and environmental health. Part A* **2004,** *67* (2), 153-
777 61.http://dx.doi.org/10.1080/15287390490264794

778 [47] Wik, J. A.; Skålhegg, B. S., T Cell Metabolism in Infection. *Frontiers in immunology* **2022,** *13*,
779 840610.http://dx.doi.org/10.3389/fimmu.2022.840610

[48] Baba, Y.; Kuroiwa, A.; Uitti, R. J.; Wszolek, Z. K.; Yamada, T., Alterations of T-lymphocyte populations in Parkinson disease. *Parkinsonism & related disorders* **2005,** *11* (8), 493-8.http://dx.doi.org/10.1016/j.parkreldis.2005.07.005

[49] Riahi, B.; Rafatpanah, H.; Mahmoudi, M.; Memar, B.; Brook, A.; Tabasi, N.; Karimi, G., Immunotoxicity of paraquat after subacute exposure to mice. *Food and chemical toxicology : an international journal published for the British Industrial Biological Research Association* **2010,** *48* (6), 1627-31.http://dx.doi.org/10.1016/j.fct.2010.03.036

[50] Goldim, M. P. S.; Della Giustina, A.; Petronilho, F., Using Evans Blue Dye to Determine Blood-Brain Barrier Integrity in Rodents. *Current protocols in immunology* **2019,** *126* (1), e83.http://dx.doi.org/10.1002/cpim.83

[51] Waisman, A.; Hauptmann, J.; Regen, T., The role of IL-17 in CNS diseases. *Acta neuropathologica* **2015,** *129* (5), 625-37.http://dx.doi.org/10.1007/s00401-015-1402-7

[52] Shi, Y.; Wei, B.; Li, L.; Wang, B.; Sun, M., Th17 cells and inflammation in neurological disorders: Possible mechanisms of action. *Frontiers in immunology* **2022,** *13*, 932152.http://dx.doi.org/10.3389/fimmu.2022.932152

[53] Beurel, E.; Harrington, L. E.; Jope, R. S., Inflammatory T helper 17 cells promote depression-like behavior in mice. *Biological psychiatry* **2013,** *73* (7), 622-30.http://dx.doi.org/10.1016/j.biopsych.2012.09.021

[54] Gu, C.; Wu, L.; Li, X., IL-17 family: cytokines, receptors and signaling. *Cytokine* **2013,** *64* (2), 477-85.http://dx.doi.org/10.1016/j.cyto.2013.07.022

[55] Huppert, J.; Closhen, D.; Croxford, A.; White, R.; Kulig, P.; Pietrowski, E.; Bechmann, I.; Becher, B.; Luhmann, H. J.; Waisman, A.; Kuhlmann, C. R., Cellular mechanisms of IL-17-induced blood-brain barrier disruption. *FASEB journal : official publication of the Federation of American Societies for Experimental Biology* **2010,** *24* (4), 1023-34.http://dx.doi.org/10.1096/fj.09-141978

[56] Kebir, H.; Kreymborg, K.; Ifergan, I.; Dodelet-Devillers, A.; Cayrol, R.; Bernard, M.; Giuliani, F.; Arbour, N.; Becher, B.; Prat, A., Human TH17 lymphocytes promote blood-brain barrier disruption and central nervous system inflammation. *Nature medicine* **2007,** *13* (10), 1173-5.http://dx.doi.org/10.1038/nm1651

Supplementary Files

This is a list of supplementary files associated with this preprint. Click to download.

- Figuresupplements.docx